第 32 卷第 1 期
2016 年 1 月

无 机 化 学 学 报
CHINESE JOURNAL OF INORGANIC CHEMISTRY

Vol.32 No.1
175-183

由芳香羧酸和 1,3,5-三咪唑基苯为配体构筑的锌、镉配合物的合成、结构和荧光性质

刘光祥

(南京市新型功能材料重点实验室,南京晓庄学院化学系,南京 211171)

摘要: 通过水热法得到了 2 个配位聚合物{[Zn(timb)(BTEC)$_{0.5}$]·H_2O}$_n$(**1**)和{[Cd(timb)(DPA)]·H_2O}$_n$(**2**)(timb=1,3,5-三咪唑基苯,H_4BTEC=均苯四甲酸,H_2DPA=2,2-联苯二甲酸),对它们进行了元素分析、红外光谱分析,并利用 X 射线衍射测定了它们的单晶结构。配合物 **1** 属于三斜晶系,$P\bar{1}$ 空间群。配合物 **2** 属于单斜晶系,$C2/c$ 空间群。配合物 **1** 拥有一个不寻常的三维框架结构,其拓扑为$(4.6^3\cdot8^6)_2(4^2\cdot8^4)(6^3)_2$;而配合物 **2** 具有一维单层纳米管结构。结果说明了金属离子和有机羧酸配体在配合物组装过程中起着非常重要的作用。此外,在室温下对 2 个配合物进行了荧光性质分析。

关键词: 配位聚合物; 三咪唑配体; 芳香羧酸配体; 晶体结构; 荧光性质
中图分类号: O614.24$^+$1; O614.24$^+$2 **文献标识码**: A **文章编号**: 1001-4861(2016)01-0175-09
DOI: 10.11862/CJIC.2016.024

Syntheses, Crystal Structures and Luminescent Properties of Zinc(Ⅱ) and Cadmium(Ⅱ) Coordination Polymers Constructed by Aromatic Carboxylates and 1,3,5-Tris(imidazol-1-yl)benzene

LIU Guang-Xiang

(*Key Laboratory of Advanced Functional Materials of Nanjing, Department of Chemistry, Nanjing Xiaozhuang University, Nanjing* 211171, *China*)

Abstract: Two coordination polymers, namely {[Zn(timb)(BTEC)$_{0.5}$]·H_2O}$_n$ (**1**) and {[Cd(timb)(DPA)]·H_2O}$_n$ (**2**), have been obtained by the reaction of metal salt (zinc nitrate or cadmium nitrate), 1,3,5-tris(imidazol-1-yl)benzene (timb) with two aromatic carboxylic acids, 1,2,4,5-benzenetetracarboxylic acid (H_4BTEC) and diphenic acid (H_2DPA). They were characterized by IR spectroscopy, elemental analysis and single-crystal X-ray diffraction. Complex **1** crystallizes in triclinic, space group $P\bar{1}$ with a=0.991 32(9) nm, b=1.018 23(10) nm, c=1.112 45(11) nm, α=81.479 0(10)°, β=65.613 0(10)°, γ=62.318 0(10)°. Complex **2** belongs to monoclinic, space group $C2/c$ with a=2.633 0(2) nm, b=0.841 96(8) nm, c=2.353 5(2) nm, β=98.027 0(10)°. Structural analyses reveal that complex **1** exhibits a novel three-dimensional (3D) (3,4,5)-connected framework with an unusual $(4.6^3\cdot8^6)_2(4^2\cdot8^4)(6^3)_2$ topology, whereas complex **2** possesses a one-dimensional (1D) single-wall metal-organic nanotube based on double helical chains. The results show that the nature of metal ions and the carboxylic building blocks play an important role in the formation of complexes with diverse structures. The luminescent properties of two complexes have also been investigated. CCDC: 1422833, **1**; 1422832, **2**.

Keywords: coordination polymer; tris(imidazole) ligands; polycarboxylate; crystal structure; luminescence

收稿日期:2015-09-28。收修改稿日期:2015-11-07。
国家自然科学基金资助项目(No.21271106)和江苏省“333 工程”培养基金资助项目。
E-mail:njuliugx@126.com

0 Introduction

The field of coordination polymers (CPs) material has undergone flourishing development in the past few years. The unique features of this type of materials, such as tunable structures, diversiform topologies, as well as potential applications in many useful areas, have made it a hot research topic for the scientist worldwide, especially for those who work in the field of crystal engineering[1-8]. In general, the applications of CPs are directly related to their structural features. Therefore, the development of new synthetic strategies to achieve CPs with targeted structures and properties has become a great challenge. Although porous CPs can be synthesized using multidentate ligands, their final structural topologies are highly influenced by several factors, including metal-ligand ratio, pH value, solvent, temperature, as well as the oxidation state of the metal ion[9-13]. In particular, the rational selection of organic ligands or co-ligands according to their lengths, rigidities, coordination modes and functional groups provides a possibility for the assembly of structurally controllable CPs[14-17].

Among the various types of organic ligands, imidazole and its derivatives are often employed to fabricate CPs because of their strong coordination abilities and relatively versatile coordination geometries [18-21]. The rigid tripodal ligand 1,3,5-tris (imidazol-1-yl)benzene (timb) has previously been justified as an efficient and versatile organic building unit for construction of coordination architectures[22-25]. For timb, the three imidazole groups can rotate with different dihedral angles so as to satisfy the demands of the coordination environments of the central metals in the assembly processes, producing favored arrangements with beautiful architectures [26-27]. More importantly, recent studies indicate that utilizing mixed ligands is an effective route to construct intriguing CPs with attractive topological structures[28-31]. Such a dual-ligand strategy offers great promise for the construction of target frameworks with high complexities due to the presence of distinct donors which can coordinate with metal centers through different coordination modes. With a view to develop possible synthetic strategies, the employment of mixed N- and O-donor ligands would be a feasible method to build coordination architectures with interesting topologies and remarkable functionalities [32-36]. As is known, polycarboxylate ligands are excellent co-ligands for the construction of highly connected, different dimensional frameworks due to their versatile bridging modes. However, investigation of the timb-carboxylate mixed-ligand system remains largely unexplored. Thus, the development of comprehensive research on this topic is necessary. Considering all of the above-mentioned, we chose timb and two co-ligands, 1,2,4,5-benzenetetracarboxylic acid (H_4BTEC) and diphenic acid (H_2DPA) to prepare CPs, and obtained two new coordination polymers with intriguing structures, namely, $\{[Zn(timb)(BTEC)_{0.5}]\cdot H_2O\}_n$ (**1**) and $\{[Cd(timb)(DPA)]\cdot H_2O\}_n$ (**2**). Herein, we report their syntheses, crystal structures and luminescent properties.

1 Experimental

1.1 Materials and general methods

All the reagents and solvents for syntheses and analyses were purchased from Sigma or TCI and employed as received without further purification. The timb ligand was synthesized according to the reported method [37]. Elemental analyses (C, H and N) were performed on a Vario EL III elemental analyzer. Infrared spectra were performed on a Nicolet AVATAR-360 spectrophotometer with KBr pellets in the 4 000~400 cm^{-1} region. The luminescent spectra for the powdered solid samples were measured at room temperature on a Horiba FluoroMax-4P-TCSPC fluorescence spectrophotometer with a xenon arc lamp as the light source. In the measurements of emission and excitation spectra the pass width is 5 nm. All the measurements were carried out under the same experimental conditions.

1.2 Synthesis of $\{[Zn(timb)(BTEC)_{0.5}]\cdot H_2O\}_n$ (1)

A mixture containing $Zn(NO_3)_2\cdot 6H_2O$ (59.5 mg, 0.2 mmol), H_4BTEC (25.4 mg, 0.1 mmol), timb (55.2 mg, 0.2 mmol) and $LiOH\cdot H_2O$ (16.8 mg, 0.4 mmol) in

15 mL of deionized water was sealed in a 25 mL Teflon lined stainless steel container and heated at 140 ℃ for 3 days. Colorless block crystals of **1** were collected by filtration and washed with water and ethanol several times with a yield of 41% based on timb ligand. Anal. Calcd. for $C_{20}H_{15}N_6O_5Zn$ (%): C, 49.55; H, 3.12; N, 17.34. Found (%): C, 49.52; H, 3.13; N, 17.35. IR spectrum (cm^{-1}): 3 481(br), 3 185 (w), 1 612 (s), 1 563 (s), 1 519 (s), 1 421 (m), 1 389 (s), 1 319 (m), 1 264 (m), 1 109 (m), 1 077 (s), 1 021 (m), 982 (m), 823 (m), 756 (m), 657 (m), 586 (w).

1.3 Synthesis of $\{[Cd(timb)(DPA)]\cdot H_2O\}_n$ (2)

Complex **2** was prepared by a process similar to that yielding complex **1** by using $Cd(NO_3)_2\cdot 4H_2O$ (30.8 mg, 0.1 mmol), H_2DPA (24.2 mg, 0.1 mmol), timb (27.6 mg, 0.1 mmol) and $LiOH\cdot H_2O$ (8.4 mg, 0.2 mmol) in 15 mL of deionized water. Colorless platy crystals of **2** were collected by filtration and washed with water and ethanol several times with a yield of 53% based on timb ligand. Anal. Calcd. for $C_{29}H_{22}N_6O_5Cd$ (%): C, 53.84; H, 3.43; N, 12.99. Found (%): C, 53.82; H, 3.44; N, 12.98. IR spectrum (cm^{-1}): 3 450 (br), 3 130 (w), 1 559 (s), 1 521 (s), 1 444 (s), 1386 (s), 1 240 (w), 1 169 (m), 1 079 (m), 931 (w), 822 (w), 766 (m), 653 (w), 556 (w).

1.4 X-ray crystallography

Two single crystals with dimensions of 0.22 mm×0.16 mm×0.14 mm for **1** and 0.26 mm×0.22 mm×0.12 mm for **2** were mounted on glass fibers for measurement, respectively. X-ray diffraction intensity data were collected on a Bruker APEX Ⅱ CCD diffractometer equipped with a graphite-monochromatic Mo-$K\alpha$ radiation (λ=0.071 073 nm) using the φ-ω scan mode at 293 (2) K. Data reduction and empirical absorption correction were performed using the SAINT and SADABS program [38], respectively. The structures were solved by the direct method using SHELXS-97[39] and refined by full-matrix least squares on F^2 using SHELXL-97 [40]. All of the non-hydrogen atoms were refined anisotropically. The hydrogen atoms of the organic ligands were refined as rigid groups. The hydrogen atoms of the solvent water molecules were located from difference Fourier maps, then restrained at fixed positions and refined isotropically. The details of the crystal parameters, data collection and refinement for **1** and **2** are summarized in Table 1, and selected bond lengths and angles with their estimated standard deviations are listed in Table 2.

CCDC: 1422833, **1**; 1422832, **2**.

Table 1　Crystal data and structure refinement for 1 and 2

Formula	$C_{20}H_{15}N_6O_5Zn$	$C_{29}H_{22}N_6O_5Cd$
Formula weight	484.75	562.26
Crystal system	Triclinic	Monoclinic
Space group	$P\bar{1}$	$C2/c$
a / nm	0.991 32(9)	2.633 0(2)
b / nm	1.018 23(10)	0.841 96(8)
c / nm	1.112 45(11)	2.353 5(2)
α / (°)	81.479 0(10)	90
β / (°)	65.613 0(10)	98.027 0(10)
γ / (°)	62.318 0(10)	90
V / nm^3	0.904 32(15)	5.166 3(8)
Z	2	8
D_c / ($g\cdot cm^{-3}$)	1.780	1.663
Absorption coefficient / mm	1.411	0.899
θ range / (°)	2.26~25.50	2.50~25.50
F(000)	494	2 608
Reflections collected	6 956	15 737

Continued Table 1

Independent reflections	3 346(R_{int}=0.018 9)	4 765 (R_{int}=0.174 7)
Reflections observed [$I>2\sigma(I)$]	2 997	4 228
Data, restraints, parameters	3 346, 2, 297	4 765, 1, 370
Goodness-of-fit on F^2	1.091	1.060
R_1, wR_2 [$I>2\sigma(I)$]	0.046 8, 0.132 1	0.047 5, 0.131 6
R_1, wR_2 (all data)	0.052 1, 0.136 0	0.055 3, 0.144 3
Largest difference peak and hole / (e·nm^{-3})	573 and −832	1 021 and −1 035

Table 2 Selected bond lengths(nm) and angles(°) for 1 and 2

		1			
Zn(1)-O(2)	0.206 5(3)	Zn(1)-N(5)^{ii}	0.213 4(3)	Zn(1)-N(1)	0.211 6(3)
Zn(1)-O(4)^{iii}	0.219 2(3)	Zn(1)-N(3)^{i}	0.212 3(3)	Zn(1)-O(3)^{iii}	0.224 4(3)
O(2)-Zn(1)-N(1)	96.53(12)	N(3)i-Zn(1)-O(4)^{iii}	89.79(12)	O(2)-Zn(1)-N(3)^{i}	84.04(12)
N(5)ii-Zn(1)-O(4)^{iii}	151.30(12)	N(1)-Zn(1)-N(3)i	178.76(12)	O(2)-Zn(1)-O(3)^{iii}	168.04(11)
O(2)-Zn(1)-N(5)^{ii}	98.15(12)	N(1)-Zn(1)-O(3)^{iii}	86.64(12)	N(1)-Zn(1)-N(5)^{ii}	95.87(13)
N(3)i-Zn(1)-O(3)^{iii}	92.58(12)	N(3)i-Zn(1)-N(5)^{ii}	85.13(13)	N(5)ii-Zn(1)-O(3)^{iii}	92.97(11)
O(2)-Zn(1)-O(4)^{iii}	109.40(11)	O(4)iii-Zn(1)-O(3)^{iii}	59.01(10)	N(1)-Zn(1)-O(4)^{iii}	88.98(12)
		2			
Cd(1)-O(3)^{i}	0.223 8(4)	Cd(1)-O(2)	0.230 1(3)	Cd(1)-N(3)^{ii}	0.225 5(2)
Cd(1)-O(1)	0.242 0(3)	Cd(1)-N(1)	0.226 6(3)	Cd(1)-O(4)^{i}	0.261 2(4)
O(3)i-Cd(1)-N(3)^{ii}	109.65(13)	N(1)-Cd(1)-O(1)	106.41(11)	O(3)^{i}-Cd(1)-N(1)	90.24(12)
O(2)-Cd(1)-O(1)	54.37(11)	N(3)^{ii}-Cd(1)-N(1)	115.34(10)	O(3)^{i}-Cd(1)-O(4)^{i}	52.49(12)
O(3)i-Cd(1)-O(2)	159.46(12)	N(3)^{ii}-Cd(1)-O(4)^{i}	83.23(10)	N(3)^{ii}-Cd(1)-O(2)	87.65(11)
N(1)-Cd(1)-O(4)^{i}	142.70(11)	N(1)-Cd(1)-O(2)	92.18(11)	O(2)-Cd(1)-O(4)^{i}	121.98(11)
O(3)i-Cd(1)-O(1)	105.47(13)	O(1)-Cd(1)-O(4)^{i}	85.29(10)	N(3)^{ii}-Cd(1)-O(1)	124.09(11)

Symmetry code: ^{i} x+1, y−1, z−1; ^{ii} x+1, y, z−1; ^{iii} −x+2, −y, −z+1 for **1**; ^{i} x, y+1, z; ^{ii} −x, y−1, −z+1/2 for **2**

2 Results and discussion

2.1 Crystal structure description

The single-crystal diffraction analysis indicates that complex **1** crystallized in a triclinic manner with space group $P\bar{1}$. There are one Zn(Ⅱ) ion, one timb ligand, half of BTEC ligand lying on inversion center, and one lattice water molecule in one asymmetric unit of **1**. The coordination environment around the Zn(Ⅱ) ion is exhibited in Fig.1 along with the atom numbering scheme. Each Zn(Ⅱ) ion is six-coordinated by three oxygen atoms from two different $BTEC^{2-}$ anions and three nitrogen atoms from three individual timb ligands to form a distorted octahedral geometry and its basal plane is occupied by three oxygen atoms, O2, O3^{iii} and O4^{iii}, and one nitrogen atom, N5^{ii}, while the apical position is occupied by two nitrogen atoms (N1 and N3^{i}). The Zn-O bond lengths are in the range of 0.206 5(3)~0.224 4(3) nm, and the Zn-N bond lengths are 0.211 6(3)~0.213 4(3) nm. The coordination angles around Zn ion are in the range of 59.01(10)~178.76(12)°.

Each timb ligand in turn connects three Zn(Ⅱ) ions which form a triangle with edge lengths (Zn…Zn) of 1.018 2, 1.144 4 and 1.320 7 nm, respectively. The three imidazolyl rings are inclined to the phenyl ring with angles of 9.93(1)°, 33.52(1)° and 35.22(1)°, respectively. As shown in Fig.2, each Zn(Ⅱ) ion

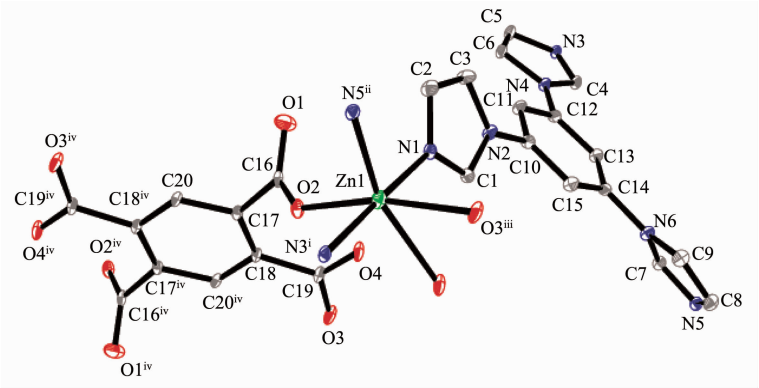

Hydrogen atoms and lattice water molecule are omitted for clarity; Symmetry code: [i] $x+1, y-1, z-1$; [ii] $x+1, y, z-1$; [iii] $-x+2, -y, -z+1$; [iv] $3-x, -y, 1-z$

Fig.1　Coordination environment of Zn(Ⅱ) in complex **1** with thermal ellipsoids at 30% probability

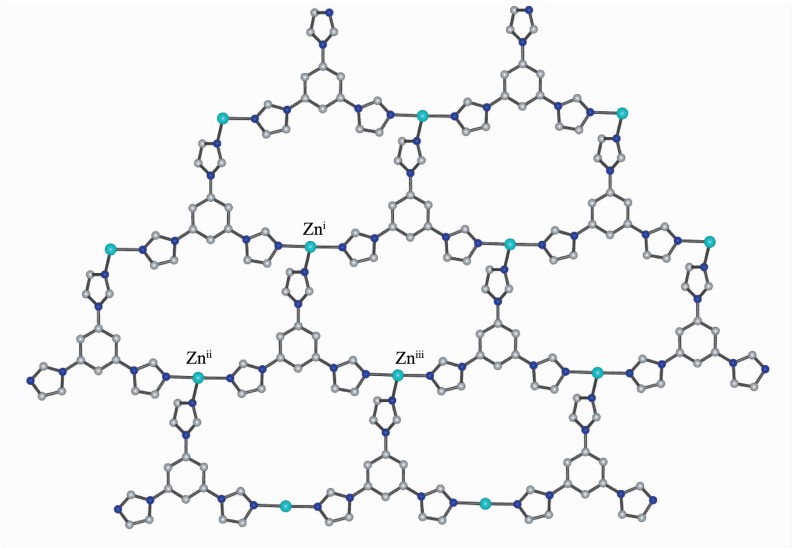

Symmetry code: [i] x, y, z; [ii] $x+1, y, z-1$; [iii] $x, y+1, z$

Fig.2　Ball-stick representation of the Zn-timb sheet in **1**

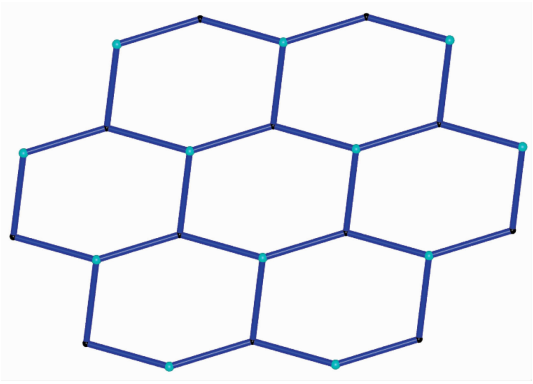

Fig.3　Schematic representation of the 2D (6,3) framework of **1**

connects three timb ligands and each timb ligand connects three Zn(Ⅱ) ions, such a coordination mode makes the complex a 2D network with honeycomb structure, and a schematic drawing is shown in Fig.3. $BTEC^{4-}$ anions adopt monodentate and bidentate chelate coordination modes and connect the Zn-timb

layers as pillars to generate a 3D structure (Fig.4). If the Zn(Ⅱ) ion is considered as a five-connected node (connecting to two $BTEC^{4-}$ anions and three timb ligands), the timb ligand can be considered as a three-connected node (connecting to three Zn(Ⅱ) ions), and the $BTEC^{4-}$ ligand can be considered as a four-connected node (connecting to four Zn(Ⅱ) ions). The structure of **1** can be classified as a rare trinodal (3,4,5)-connected $(4.6^3\cdot8^6)_2(4^2\cdot8^4)(6^3)_2$ topology (Fig.5). As far as we know, this topology has not previously been reported in the literature. In order to minimize the space void and stabilize the framework, the potential void cavities are occupied by the uncoordinated water molecules.

X-ray single-crystal diffraction analysis reveals that **2** is an independent 1D single-wall metal-organic nanotube. It crystallizes in the monoclinic crystal system with space group of *C*2/*c*. The asymmetric unit consists of one Cd(Ⅱ) ion, one timb ligand, one DPA dianion, and one uncoordinated water molecule. As depicted in Fig.6, each Cd(Ⅱ) ion is six-coordinated by two nitrogen atoms from two timb ligands and four oxygen atoms from two carboxylate groups of two DPA anions in a distorted octahedral coordination environment. Its basal plane is occupied by two oxygen atoms from two different DPA ligands (O1 and $O4^{i}$) and two nitrogen atoms from two individual timb ligands (N1 and $N3^{ii}$), while the apical position is occupied by two oxygen atoms (O2 and $O3^{i}$). The Cd-O bond lengths are in the range of 0.223 8(4)~0.261 2(4) nm, and the Cd-N bond lengths are 0.225 5(2)~0.226 6(3) nm. The coordination angles around Cd ion are in the range of 52.49(12)°~159.46(12)°.

It is noteworthy that the timb ligand coordinates with two, rather than three like in **1**, Cd(Ⅱ) ions using two of its three imidazole groups, and the third one with N6 did not participate in the coordination, which has been observed previously[27]. Three dihedral angles

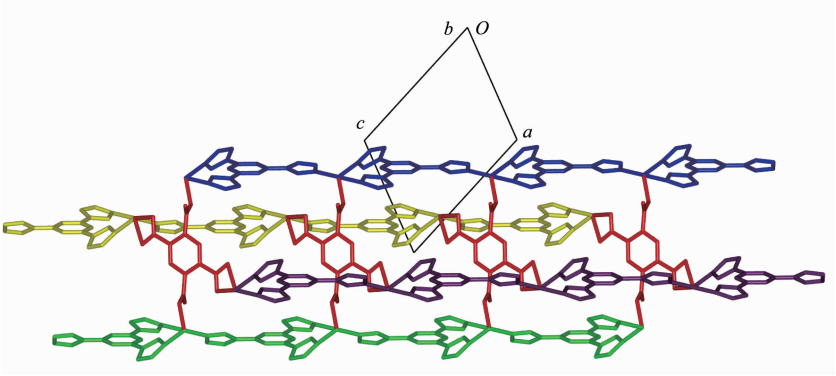

Fig.4 Stick representation of a 3D structure of **1** along the *b*-axis

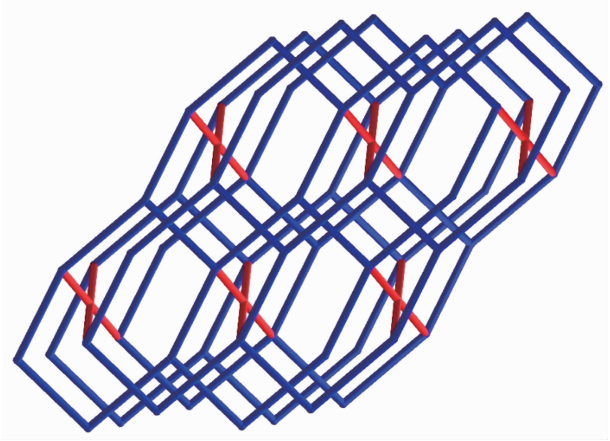

Fig.5 Schematic view of the $(4.6^3\cdot8^6)_2(4^2\cdot8^4)(6^3)$ topology of **1**

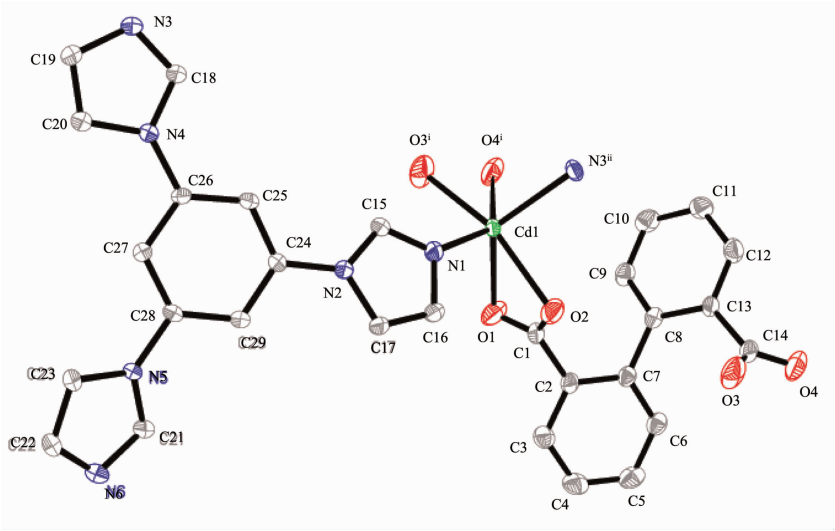

Hydrogen atoms and lattice water molecule were omitted for clarity; Symmetry code: [i] x, $y+1$, z; [ii] $-x$, $y-1$, $-z+1/2$

Fig.6　Coordination environments of the Cd(Ⅱ) atoms in **2** with the ellipsoids drawn at the 30% probability level

formed between the central phenyl ring and three terminal imidazole groups are 20.63 (1)°, 34.72 (1)°, and 5.26 (1)°, respectively. The timb ligand acts as bidentate bridging ligand to bind two Cd(Ⅱ) atoms to form double helical chains (Fig.7). Both helical pitches are 1.683 9 nm. Two carboxylate groups of DPA are arranged in the opposite sites relative to the central phenyl ring, giving an *anti*-conformation, which link the Cd-timb helical chains generate an open-ended, hollow single-wall metal-organic nanotube (Fig.8) with the interior cross section size of *ca.* 0.589 nm×0.669 nm. The interior of the single-wall metal-organic nanotube is occupied by the uncoordinated water molecules. The neighboring single-wall metal-organic nanotubes are all held together by weak $\pi\cdots\pi$ stacking interaction (0.404 9(1) nm) between imidazole and phenyl ring of timb and nonclassical C-H⋯O hydrogen bonds to form a 3D supramolecular framework.

2.2　FTIR spectra

FTIR spectra revealed valuable information about the coordination modes of H_4BTEC and H_2DPA. The

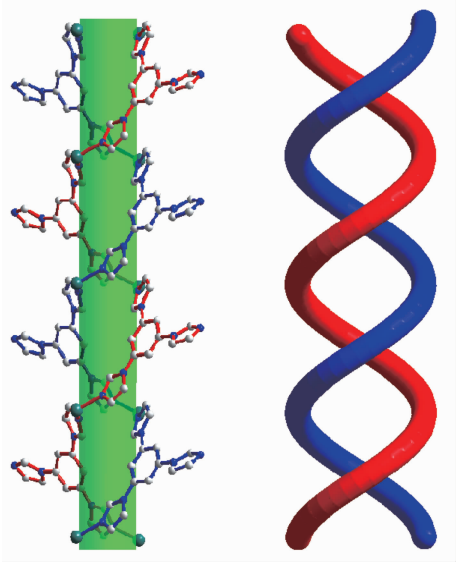

Fig.7　View of the 1D infinite double helical chains along the *b*-axis formed by timb and Cd(Ⅱ) ions

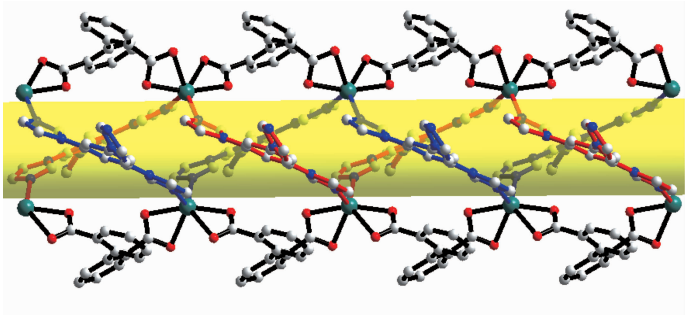

Fig.8 Ball-and-stick representations of 1D single-wall metal-organic nanotube

IR spectra of **1** and **2** show the absence of the characteristic bands at around 1 700 cm^{-1} attributed to the protonated carboxylate group, which indicates that the complete deprotonation of H_4BTEC and H_2DPA upon reaction with metal ion. The difference between asymmetric and symmetric carbonyl stretching frequencies ($\Delta\nu=\nu_{asym}-\nu_{sym}$) was used to fetch information on the metal-carboxylate binding modes. Complex **1** showed two pairs of ν_{asym} and ν_{sym} frequencies at 1 612, 1 421 ($\Delta\nu$=191 cm^{-1}) and 1 563, 1 389 cm^{-1} ($\Delta\nu$=174 cm^{-1}) for the carbonyl functionality indicating two coordination modes as observed in the crystal structure. Complex **2** showed a pairs of ν_{asym} and ν_{sym} frequencies at 1 559, 1 386 cm^{-1} ($\Delta\nu$=173 cm^{-1}) corresponding to the carbonyl functionality of dicarboxylate ligand indicating a symmetric bis (monodentate) coordination mode. OH stretching broad bands at 3 481 cm^{-1} for **1** and 3 450 cm^{-1} for **2** are attributable to the coordinated lattice water. The bands in the region of 640~1 250 cm^{-1} are attributed to the -CH- in-plane or out-of-plane bend, ring breathing, and ring deformation absorptions of benzene ring. The IR spectra also exhibit the characteristic peaks of imidazole groups at *ca.* 1 520 cm^{-1} [41].

2.3 Luminescent properties

The luminescence properties of coordination polymers with d^{10} metal centers and π-conjugated organic linkers have attracted intense interest due to their potential applications in chemical optical sensors and light-emitting devices[42-44]. Solid state photoluminescent properties of **1** and **2**, as well as those of the free ligands, were examined at ambient temperature. The free timb ligand displays photoluminescence with an emission maximum at 404 nm (λ_{ex}=340 nm), which is in accordance with previous reports[45]. Upon complexation of the organic ligands with Zn(Ⅱ)/Cd(Ⅱ) ions, intense blue emissions are observed at 408 nm for **1**, and 425 nm for **2** under excitation at 340 nm, as depicted in Fig.9. Since Zn(Ⅱ)/Cd(Ⅱ) ions are difficult to oxidize or reduce due to their d^{10} configurations, the emissions of complexes **1** and **2** are neither metal-to-ligand charge transfer (MLCT) nor ligand-to-metal charge transfer (LMCT) in nature. Thus, they may be assigned to being characteristic of intraligand charge transfer, as reported for other Zn(Ⅱ)/Cd(Ⅱ) CPs constructed from mixed N-donor and O-donor ligands[46-47]. The maximum emission peak of **1** is similar to that of the free timb ligand and the emission band of **2** is relatively red-shifted (17 nm). The differences in the emission behaviors of **1** and **2** probably derive from their distinct metal centers and varied polycarboxylate co-ligands, which may affect the rigidity of the solid-state crystal packing and further influence their luminescence emission bands.

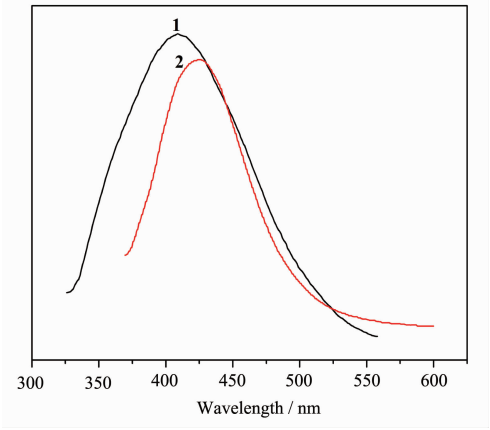

Fig.9 Solid-state photoluminescent spectra of complexes **1** and **2**

References:

[1] Du M, Li C P, Chen M, et al. *J. Am. Chem. Soc*., **2014**,**136**: 10906-10909

[2] Long J R, Yaghi O M. *Chem. Soc. Rev*., **2009**,**38**:1213-1214

[3] Liu C S, Yang X G, Hu M, et al. *Chem. Commun*., **2012**,**48**: 7459-7461

[4] Chen L, Chen Q, Wu M, et al. *Acc. Chem. Res*., **2015**,**48**: 201-210

[5] Liu K, Shi W, Cheng P. *Coord. Chem. Rev*., **2015**,289-290: 74-122

[6] Zhou H C, Kitagawa S. *Chem. Soc. Rev*., **2014**,**43**:5415-5418

[7] Du M, Li C P, Liu C S, et al. *Coord. Chem. Rev*., **2013**,**257**: 1282-1305

[8] Zhou H C, Long J R, Yaghi O M. *Chem. Rev*., **2012**,**112**: 673-674

[9] Guo X M, Guo H D, Zou H Y, et al. *CrystEngComm*, **2013**, **15**:9112-9120

[10]Zhao F H, Jing S, Che Y X, et al. *CrystEngComm*, **2012**,**14**: 4478-4485

[11]Shen L, Gray D, Masel R I, et al. *CrystEngComm*, **2012**,**14**: 5145-5147

[12]Stock N, Biswas S. *Chem. Rev*., **2012**,**112**:933-969

[13]Guo H D, Guo X M, Zou H Y, et al. *CrystEngComm*, **2014**, **16**:7459-7468

[14]Zhou K, Jiang F L, Chen L, et al. *Chem. Commun*., **2012**, **48**:12168-12170

[15]Hu F L, Wang S L, Wu B, et al. *CrystEngComm*, **2014**,**16**: 6354-6363

[16]Pan M, Su C Y. *CrystEngComm*, **2014**,**16**:7847-7859

[17]Ding J G, Yin C, Zheng L Y, et al. *RSC Adv*., **2014**,**4**: 24594-24600

[18]Yao X Q, Pan Z R, Hu J S, et al. *Chem. Commun*., **2011**, **47**:10049-10051

[19]Li S, Sun W, Wang K, et al. *Inorg. Chem*., **2014**,**53**:4541-4547

[20]Tian Y Q, Zhao Y M, Chen Z X, et al. *Chem. Eur. J*., **2007**, **13**:4146-4154

[21]Phan A, Doonan C J, Uribe-Romo F J, et al. *Acc. Chem. Res*., **2010**,**43**:58-67

[22]Mukherjee S, Samanta D, Mukherjee P S. *Cryst. Growth Des*., **2013**,**13**:5335-5343

[23]Xu Z Z, Sheng T L, Wang Y L, et al. *CrystEngComm*, **2015**,**17**:2004-2012

[24]Wang H, Yi F Y, Dang S, et al. *Cryst. Growth Des*., **2014**, **14**:147-156

[25]Hua J A, Zhao Y, Liu Q, et al. *CrystEngComm*, **2014**,**16**: 7536-7546

[26]Wang L, Yan Z H, Xiao Z, et al. *CrystEngComm*, **2013**, **15**:5552-5560

[27]Sun D, Yan Z H, Blatov V A, et al. *Cryst. Growth Des*., **2013**,**13**:1277-1289

[28]Hauptvogel I M, Bon V, Grünker R, et al. *Dalton Trans*., **2012**,**41**:4172-4179

[29]Kim D, Lah M S. *CrystEngComm*, **2013**,**15**:9491-9498

[30]Cao T, Peng Y, Liu T, et al. *CrystEngComm*, **2014**,**16**: 10658-10673

[31]Li Y W, Li D C, Xu J, et al. *Dalton Trans*., **2014**,**43**:15708-15712

[32]Jiang H L, Tatsu Y, Lu Z H, et al. *J. Am. Chem. Soc*., **2010**,**132**:5586-5587

[33]Liu X M, Lin R B, Zhang J P, et al. *Inorg. Chem*., **2012**,**51**: 5686-5692

[34]Han L W, Lu J, Lin Z J, et al. *CrystEngComm*, **2014**,**16**: 1749-1754

[35]Kongpatpanich K, Horike S, Sugimoto M, et al. *Chem. Commun*., **2014**,**50**:2292-2294

[36]Das M C, Guo Q, He Y, et al. *J. Am. Chem. Soc*., **2012**, **134**:8703-8710

[37]Zhao W, Song Y, Okamura T A, et al. *Inorg. Chem*., **2005**, **44**:3330-3336

[38]Sheldrick G M. *SADABS, Program for Empirical Absorption Correction of Area Detector Data*, University of Göttingen, Germany, **1996**.

[39]Sheldrick G M. *SHELXS*-97, *Program for Crystal Structure Solution*, University of Göttingen, Germany, **1997**.

[40]Sheldrick G M. *SHELXL*-97, *Program for the Refinement of Crystal Structure*, University of Göttingen, Germany, **1997**.

[41]Nakamoto K. *Infrared and Raman Spectra of Inorganic and Coordinated Compounds*. *5th Ed*. New York: Wiley & Sons, **1997**.

[42]Zhang S R, Du D Y, Qin J S, et al. *Chem. Eur. J*., **2014**,**20**: 3589-3594

[43]Zhang M, Feng G, Song Z, et al. *J. Am. Chem. Soc*., **2014**, **136**:7241-7244

[44]Zhou X, Li P, Shi Z, et al. *Inorg. Chem*., **2012**,**51**:9226-9231

[45]Li L, Fan J, Okamura T A, et al. *Supramol. Chem*., **2004**,**16**: 361-370

[46]Coropceanu E B, Croitor L, Siminel A V, et al. *Polyhedron*, **2014**,**75**:73-80

[47]Sie M J, Chang Y J, Cheng P W, et al. *CrystEngComm*, **2012**,**14**:5505-5516